

# Effects of disorder on the Raman line-shape in $\text{ZrO}_2$

L. A. Falkovsky \*

*Landau Institute for Theoretical Physics, 119337 Moscow, Russia*

## Abstract

Experimental data obtained by Lugi and Clarke [J. Am. Ceram. Soc., to be published] are compared to the theory describing disorder effects on optical phonons. Sharpening and vanishing of the asymmetry of the Raman lines after annealing are attributed to a decrease in short-range disorder. The parameters of disorder (such as the phonon-defect coupling and the correlation length) are defined in the comparison.

arXiv:cond-mat/0509534v1 [cond-mat.mtrl-sci] 21 Sep 2005

---

\* e-mail: falk@itp.ac.ru

## I. INTRODUCTION

Raman scattering has been used for years to measure the center-zone phonon frequencies. But it was understood quite recently that studies of the Raman line shape can also provide widespread information relative to disorder, for instance, the isotopic compositions [1], the stacking faults [2]-[3], the strain fluctuations near interfaces [4], and so on. The phonon scattering processes by defects of various types result in increasing the phonon relaxation rate and consequently the Raman line width.

A novel field of Raman spectroscopy, the transformation kinetics, was put forward by Lughii and Clarke [5]. They investigated the phase transformations of yttria-stabilized zirconia. Zirconia  $\text{ZnO}_2$  has the wide range of applications, including traditional structural refractories, fuel cells, and electronic devices such as oxygen sensors. Because of these technological implications, the characterization of zirconia is of particular interest. Zirconia has three zero-pressure polymorphs: the high-temperature cubic ( $c$ ) phase (stable between 2570 K and the melting temperature 2980 K), the tetragonal ( $t$ ) phase (stable between 1400 and 2570 K), and monoclinic ( $m$ ) phase below 1400 K.

The unit cell of the  $c$  phase contains one formula unit. There is only one triply degenerated Raman active mode at  $640 \text{ cm}^{-1}$  [6],[7]. From the symmetry analysis, it is suggested [8]-[9] that the  $c - t$  transformation of  $\text{ZnO}_2$  results from a condensation of the Brillouin zone boundary phonons. Indeed, it was found in the model calculation [10],[11] of phonon curves, that the phonon frequency  $\omega(X_2^-)$  of the  $c$ -phase is close to zero. The volume of the elementary cell is doubled in the  $c - t$  transformation. In the  $t$  phase, there are six Raman active modes [12], [13] (their frequencies are given in Table).

In the work [5], zirconia coatings were obtained by electron beam evaporation and then annealed. The X-ray diffraction and Raman spectroscopy measurements were performed before and after annealing. They give a possibility to control the phase transformation in the samples. The obtained results are very interesting because they demonstrate the gigantic effect of annealing on both the width and asymmetry of the Raman line.

In the present paper we compare the results [5] with the theory [14] describing the disorder effect on the optical phonons. In Sec. II, a sketch of the theory is presented. The comparison of the theory with the experiment [5] are given in Sec. III. In Sec. IV, concluding remarks are summarized.

## II. THEORETICAL BACKGROUND: PHONON ELASTIC SCATTERING BY STATIC DISORDER

The scattering of phonons by disorder (defects or strain fluctuations) results in the phonon width and shift (see [15] for review ). To estimate the effect of disorder we can use the quantum-mechanical formula [16]:

$$\Gamma(\omega, \mathbf{q}) - \Gamma^{\text{nat}} \propto \pi c_d \sum_{\mathbf{k}} |v(\mathbf{k} - \mathbf{q})|^2 \delta(\omega_0^2 \pm s^2 k^2 - \omega^2), \quad (1)$$

giving the phonon width as a function of the frequency and wave vector. Here  $c_d$  is the concentration of defects,  $v(\mathbf{k} - \mathbf{q})$  is the phonon-defect interaction,  $\omega$  is the phonon frequency in the initial state,  $\omega_0^2 \pm s^2 k^2$  is the squared phonon frequency in the final state (the "+" sign if the phonon branch has a minimum at  $\omega_0$  and the "-" sign for the maximum), and  $\delta(x)$  is the Dirac  $\delta$ -function expressing the conservation law in the phonon elastic scattering. The summation is performed over the 3-dimensional wave vector  $\mathbf{k}$  in the case of phonon scattering by the point defects under consideration.

Let us consider the short-range defects with the interaction having the form of the  $\delta$ -function in the real space. Then, the potential  $v$  is independent of the wave vector, i.e.  $v(\mathbf{k} - \mathbf{q}) = v_0$  with a constant value  $v_0$ , and the integration can be done explicitly. For the phonon minimum, the contribution of the scattering by defects appears only in the region  $\omega^2 > \omega_0^2$ :

$$\Gamma(\omega) = \Gamma^{\text{nat}} + \frac{c_d}{4\pi\omega_0 s^3} |v_0|^2 \sqrt{\omega^2 - \omega_0^2}. \quad (2)$$

In the case of the phonon branch maximum, we have the disorder contribution only if  $\omega^2 < \omega_0^2$ .

Expression (2) has a transparent physical meaning: the phonon elastic scattering from defects produces some phonon width in that frequency range, where the appropriate final phonon states occur. For instance, in the case of the minimum of the phonon branch at  $\omega = \omega_0$ , the final phonon states are only for  $\omega > \omega_0$ . Of course, this effect manifests itself as a line asymmetry in the Raman light scattering on phonons. As a result, the high-frequency wing of the line drops more slowly (than the low-frequency one) for a phonon branch having the minimum at the center of the Brillouin zone.

I should emphasize that the frequency dependence of the phonon-defect width is determined by the dimensionality of defects. As we see from Eq. (2), this is a square-root

dependence for point defects. In the case of linear defects such as dislocations (or the plane defects – crystallite boundaries or stacking faults), we have the 2d (or 1d) integration in Eq. (1) which gives

$$\Gamma(\omega) = \Gamma^{\text{nat}} + \frac{c_l}{4\omega_0 s^2} |v_0|^2 \theta(\omega^2 - \omega_0^2), \text{ line defect}, \quad (3)$$

$$\Gamma(\omega) = \Gamma^{\text{nat}} + \frac{c_p}{4\omega_0 s} |v_0|^2 (\omega^2 - \omega_0^2)^{-1/2}, \text{ plane defect}, \quad (4)$$

where  $\theta(x)$  is the Heaviside step-function.

The singularities in Eqs. (3) - (4) as well as the weak singularity in Eq. (2) arise, because the width of final states was not taken into account. There is another shortcoming of the simple expressions (1)-(4): they do not describe the shift of the phonon frequency due to the interaction with disorder. Therefore, we have to use a more complicated technique of the Green functions [14].

The heart of the technique is the phonon self-energy

$$\Sigma(\omega) = -c_d \sum_k \frac{|v(\mathbf{k} - \mathbf{q})|^2}{\Omega^2(\omega) \pm s^2 k^2 - i\omega\Gamma(\omega) - \omega^2}. \quad (5)$$

The real functions  $\Omega(\omega)$  and  $\Gamma(\omega)$  are now themselves defined by the real and imaginary parts of the self-energy. We obtain them by solving the system of the equations

$$\Omega^2(\omega) - \omega_0^2 - i\omega[\Gamma(\omega) - \Gamma^{\text{nat}}] - c_d v(q=0) = \Sigma(\omega). \quad (6)$$

The last term (named the homogenous shift) in the left-hand side of Eq. (6) gives the phonon shift due to the averaged effect of disorder, whereas the self-energy, Eq. (5), describes the fluctuation effect of the defects. In addition to the phonon shift (inhomogeneous, depending on the frequency), the self-energy produces a phonon width. Note, that if the phonon does not interact with disorder ( $v = 0$ ), Eqs. (6) naturally give  $\Omega(\omega) = \omega_0$  and  $\Gamma(\omega) = \Gamma^{\text{nat}}$ . Next, in the Born approximation, Eqs. (5)-(6) give the simple expression, Eq. (1), for the phonon damping.

In the Raman light scattering, the wave-vector transfer  $q \sim \omega^{(i)}/c$  is determined by the wave vector of incident light,  $\omega^{(i)}$  being the incident light frequency. In the integral (5), the values of  $k \sim 1/l = \sqrt{\Gamma\omega_0}/s$  are important, where  $l$  plays the role of the phonon mean free path. The dispersion parameter  $s \sim 5 \times 10^5$  cm/s is typically of the order of the sound velocity and the width  $\Gamma$  is of the order of  $(10^{-1} \div 10^{-2})\omega_0$ . Thus, the condition  $q \ll k$  holds and we can omit  $q$  in Eq. (5).

To simplify the calculations, we assume that the potential function  $v(\mathbf{k})$  takes constant value  $v_0$  in the region  $k < 1/r_0$  and is equal to zero for  $k > 1/r_0$ . Then the parameter  $r_0$  gives the size of the region in the real space, where phonons are scattered by defects. If we consider the phonon scattering by strain fluctuations,  $r_0$  has the meaning of the correlation length of these fluctuations.

The line asymmetry is very sensitive to the relation between the parameters  $r_0$  and  $l$ . The case where  $r_0 < l$  is referred to as the short-range disorder. It is easy to verify that the line asymmetry is much larger for the short-range disorder than in the opposite case. We can rewrite the condition of the short-range disorder as

$$\pi \frac{r_0 \sqrt{\Gamma \omega_0}}{a \omega_D} < 1, \quad (7)$$

using the estimate of the Debye frequency  $\omega_D = \pi s/a$ , where  $a$  is the lattice constant.

For the point defects, the calculation of  $\Sigma(\omega)$ , Eq. (5), gives

$$\begin{aligned} \Sigma(\omega) = A \left[ b - (a_1 - ia_2) \left( \frac{1}{4} \ln \frac{(b+a_1)^2 + a_2^2}{(b-a_1)^2 + a_2^2} \right. \right. \\ \left. \left. + \frac{i}{2} \arctan \frac{b+a_1}{a_2} + \frac{i}{2} \arctan \frac{b-a_1}{a_2} \right) \right] \end{aligned} \quad (8)$$

in the case of maximum of the phonon branch and

$$\begin{aligned} \Sigma(\omega) = A \left[ -b + (a_2 + ia_1) \left( \frac{1}{4} \ln \frac{(b+a_2)^2 + a_1^2}{(b-a_2)^2 + a_1^2} \right. \right. \\ \left. \left. - \frac{i}{2} \arctan \frac{b+a_2}{a_1} - \frac{i}{2} \arctan \frac{b-a_2}{a_1} \right) \right] \end{aligned} \quad (9)$$

in the case of minimum. Here

$$\begin{aligned} a_1 &= [\Omega^2(\omega) - \omega^2 + \rho(\omega)]^{1/2} / \sqrt{2}, \\ a_2 &= [-\Omega^2(\omega) + \omega^2 + \rho(\omega)]^{1/2} / \sqrt{2}, \\ \rho(\omega) &= [(\Omega^2(\omega) - \omega^2)^2 + \omega^2 \Gamma^2(\omega)]^{1/2}, \\ b &= s/r_0, \quad A = c_d v_0^2 / 2\pi^2 s^3. \end{aligned}$$

Notice, that the dimensions are the following:  $s$  [cm  $\omega$ ],  $c_d$  [1/cm<sup>3</sup>],  $v_0$  [cm<sup>3</sup> $\omega^2$ ],  $A$  [ $\omega$ ].

Solving the system of Eqs. (5)-(6), we find the functions  $\Omega(\omega)$  and  $\Gamma(\omega)$ . Then we can calculate (see, i.e., [4]) the Raman intensity

$$I(\omega) \sim \frac{\omega \Gamma(\omega)}{[1 - \exp(-\hbar\omega/k_B T)][(\Omega^2(\omega) - \omega^2)^2 + \omega^2 \Gamma^2(\omega)]}. \quad (10)$$

Equation (10) can be applied to the Stokes lines ( $\omega > 0$ ), as well as to the anti-Stokes ones ( $\omega < 0$ ).

If  $\Omega(\omega) = \omega_0$  and  $\Gamma(\omega) = \Gamma^{\text{nat}}$  are constant, Eq. (10) gives the Lorentzian line-shape, because  $\Gamma^{\text{nat}} \ll \omega_0$ . But, as we have already seen, the non-Lorentzian line-shape is obtained if the width  $\Gamma(\omega)$  depends on  $\omega$ .

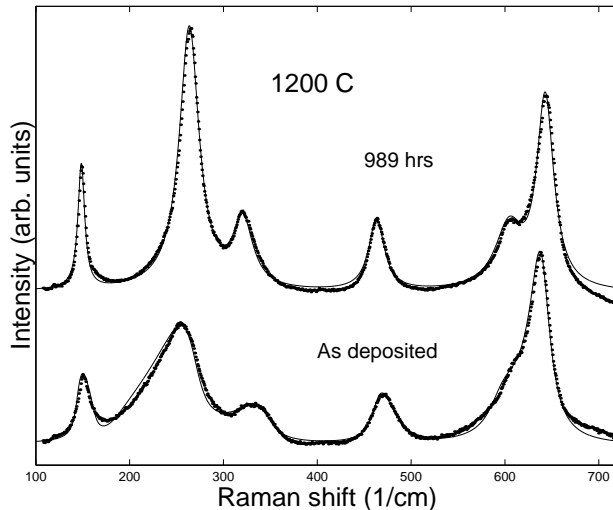


FIG. 1: Raman spectra (points - the experiment data, solid lines - the theory) from the sample in as-deposited conditions (bottom) and after annealing for 989 hrs at 1200 °C (top).

Up to this point we have considered a single phonon line. In the general case there are several lines with their positions  $\Omega_i(\omega)$  and widths  $\Gamma_i(\omega)$ . The corresponding terms have to be summarized in Eq. (10). The intervalley terms with  $v_{ij}$  could be written also in the self-energy (5). These terms are essential when the disorder removes the degeneration of branches.

### III. COMPARISON OF THE THEORY WITH THE EXPERIMENTAL DATA FOR ZIRCONIA

Two Raman spectra taken from paper [5] are shown in Fig. 1. They were recorded from two samples of yttria-stabilized (8.6 mol%  $\text{YO}_{1.5}$ ) zirconia – the first in as-deposited condition (bottom) and the second (top) annealed at 1200 °C. Narrowing and decrease of asymmetry of the lines are evident. The fit to the theory, Eqs. (8)-(9), is shown in solid lines;

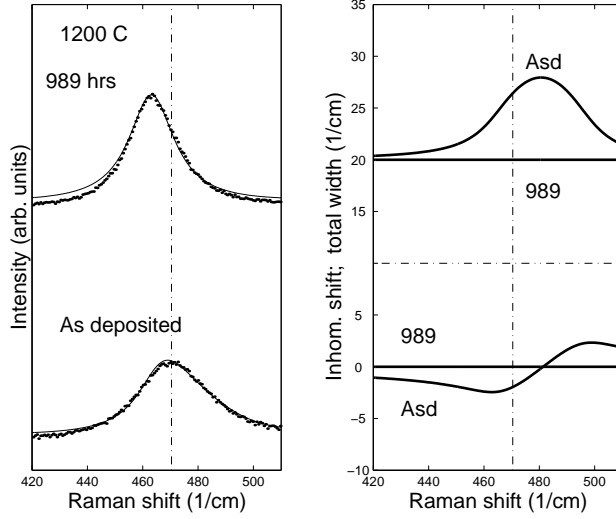


FIG. 2: Raman line  $470 \text{ cm}^{-1}$  (points - the experiment data, solid lines - the theory) from the sample in as-deposited conditions (left panel, bottom) and after annealing for 989 hrs at  $1200 \text{ }^\circ\text{C}$  (left panel, top); the peak of line from the as-deposited sample is marked by the vertical dash-dotted lines. The asymmetry of the line indicates that the phonon branch has a minimum. In the right panel, the total width  $\Gamma(\omega)$  (top) and the inhomogeneous shift  $\Omega(\omega) - \omega_0$  (bottom) are plotted versus the frequency transfer for two spectra.

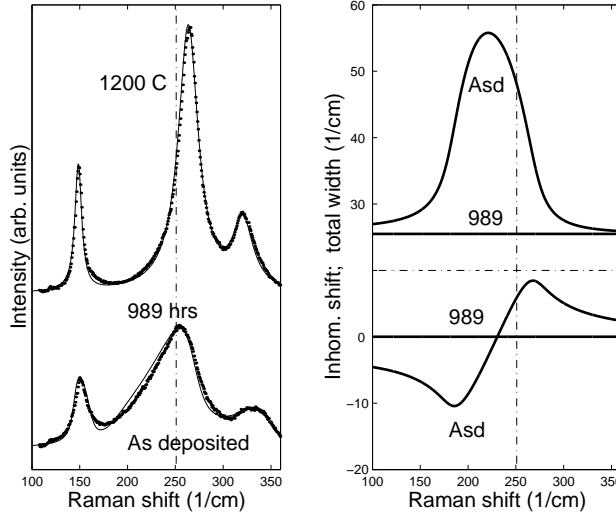


FIG. 3: Same as Fig. 2, but for the line  $250 \text{ cm}^{-1}$ . The phonon branch now has a maximum.

parameters of the fit are listed in Table. In fitting, we assume that the effect of disorder on the spectra from the sample after annealing is negligible ( $A = 0$ ). There is no information about the width of Raman lines for pure zirconia. Therefore, the line widths for the sample after annealing are referred to as the natural widths  $\Gamma^{\text{nat}}$ .

The broadening  $\Gamma - \Gamma^{\text{nat}}$  of the line for the sample in as-deposited conditions is induced by the phonon-disorder interaction determined by the parameter  $A$ . We assume, that the natural width  $\Gamma^{\text{nat}}$  of each line before annealing is equal to  $\Gamma^{\text{nat}}$  of the same line after annealing (see Table).

The line shape of spectra for the sample with disorder is determined by two factors: (i) the value of the parameter  $r_0$  and (ii) the extremum type (minimum or maximum) of the phonon branch. In Figs. 2 and 3 the results of fitting are shown in detail. The  $470.5 \text{ cm}^{-1}$  line is shown in Fig. 2, left panel. The high-frequency wing of the line from the as-deposited sample is more gentle. This corresponds to the minimum of the phonon branch. In the right panel, the width  $\Gamma(\omega)$  and the inhomogeneous shift  $(\Omega(\omega) - \omega_0)$  are plotted on the top and bottom, respectively, as functions of the frequency transfer  $\omega$ . For the sample after annealing, they are constant  $\Gamma(\omega) = \Gamma^{\text{nat}}$  and  $\Omega(\omega) = \omega_0$ .

We see that the width  $\Gamma(\omega)$  of the line from as-deposited sample increases with the frequency transfer around the line peak  $\Omega_0$ , which is marked by the dash-dotted vertical line. This resembles the square-root dependence in Eq. (2) for the minimum of the phonon branch and we use Eq. (9) in fitting. At the peak position, the width takes the value  $\Gamma_0$ ; this value is given in Table, it is slightly less than the FWHM (full-width at half-maximum) because of the frequency dependent  $\Gamma(\omega)$ .

The behavior of the  $250 \text{ cm}^{-1}$  line (see Fig. 3) from the as-deposited sample has the opposite character: the low-frequency wing drops more slowly. Then we use Eq. (8) corresponding to the maximum of the phonon branch. The asymmetry parameter  $As$  listed in Table is a difference between the right and left wings at the half-maximum. This parameter takes positive (negative) values for the phonon-branch minimum (maximum). The asymmetry parameter and the FWHM were determined for the line extracted from the total spectra with the help of the fit.

Several points can be noted in Table. First, the radius of defects (correlation radius) is about the value of the lattice parameter  $a$ . This is the case of a short-range disorder resulting in the evident asymmetry of the line shape. Second, because of disorder, the line

TABLE I: Final values obtained in fitting for spectra from the samples after annealing at 1200 °C (Ann) and as deposited (Asd): the experimental (according to [13]) phonon frequency  $\Omega_{exp}$ , the peak position  $\Omega_0$ , the peak position  $\omega_0$  including only the homogeneous shift, the total line width  $\Gamma_0$  (subscript 0 is referred to as the peak position), the natural line width  $\Gamma^{nat}$ , the line asymmetry  $As$ , the interaction parameter  $A$  (all in  $\text{cm}^{-1}$ ), the defect radius  $r_0/a$  (dimensionless), the relative intensity  $I_0$ , and the type of extremum.

line	$\Omega_{exp}$	$\Omega_0$	$\omega_0$	$\Gamma_0$	$\Gamma^{nat}$	$As$	$A$	$r_0/a$	$I_0$	extr
1 Ann	149	148.6	148.6	8.7	8.7	0	0	-	0.215	min
1 Asd		151.2	152.0	14.6	8.7	3.1	225	1.60	0.19	min
2 Ann	269	264.0	264.0	25.5	25.5	0	0	-	3.32	max
2 Asd		250.9	245.0	48.0	25.5	-23.7	225	0.73	2.55	max
3 Ann	319	321.0	321.0	26.0	26.0	0	0	-	1.15	max
3 Asd		330.4	325.0	45.0	26.0	-18.4	200	0.83	1.10	max
4 Ann	461	463.3	463.3	20.0	20.0	0	0	-	1.55	min
4 Asd		470.5	472.5	26.5	20.0	5.2	100	1.27	1.45	min
5 Ann	602	604.5	604.5	36.0	36.0	0	0	-	3.30	min
5 Asd		602.1	605.0	43.3	36.0	5.8	75	0.95	2.30	min
6 Ann	648	643.0	643.0	22.0	22.0	0	0	-	6.70	max
6 Asd		636.4	633.5	27.2	22.0	-3.9	50	0.95	7.85	max

position is slightly shifted (by less than 5 %), but the line width increases considerably. This can be understood with the help of Figs. 2 and 3 (right panels). The frequency dependence of the shift function  $\Omega(\omega) - \omega_0$  has a zero about the line peak, whereas the width function  $\Gamma(\omega)$  takes almost its maximum value.

#### IV. DISCUSSION

Lughi and Clarke explained their results in the following way. The Raman line becomes more symmetric after annealing. According to the condition (7), this means that the correlation radius of disorder in as-deposited samples must be quite small, of a few lattice

parameters. Therefore, the disorder can not be induced by the large-scale strain fluctuations, for instance, of the crystallite size (about 50 nm).

The disorder with small correlation length can be realized by  $Y^{3+}$  ions and their associated oxygen vacancies. But the concentration of yttria (8.6 mol%) before and after annealing is the same in the sample. Lughi and Clarke proposed a redistribution mechanism of the  $Y^{3+}$  ions and oxygen vacancies. They reasoned that the regions of the  $c$  phase become richer (and the  $t$  phase is more pure) in the  $Y^{3+}$  ions and oxygen vacancies in the  $t - c$  phase transformation during annealing. Because of this redistribution of defects the Raman active  $t$  phase exhibits the symmetric and narrowing Raman lines.

Considering the ions and vacancies as the point defects that scatter the long-wave optical phonons, we use Eqs. (8)-(9) in our comparison.

Finally, as can be seen from Table, the phonon-disorder interaction is larger for the low frequency lines. This interaction decreases progressively with the frequency of the lines. We conclude that the distribution of the heavier defect ions, i.e.,  $Y^{3+}$ , affects the phonon modes stronger than the disorder of oxygen vacancies.

## V. ACKNOWLEDGMENTS

I am grateful to V. Lughi and D.R. Clarke for providing their data and a copy of Ref. [5] prior to publication. The work was supported by the RFBR Grant # 04-02-17087.

- 
- [1] A. Göbel, T. Ruf, J. M. Zhang, R. Lauck, M. Cordona, Phys. Rev. B **59**, 2749 (1999).
  - [2] S. Nakashima, Y. Nakatake, H. Harima, M. Katsuno, N. Ohtani, Appl. Phys. Letts. **77**, 3612 (2000); see also S. Nakashima, H. Ohta, M Hangyo, B. Palosz, Philos. Mag. B **70**, 971 (1994).
  - [3] S. Rohmfeld, M. Hundhausen, L. Ley, Phys. Rev. B **58**, 9858 (1998).
  - [4] L. A. Falkovsky, J. M. Bluet, J. Camassel, Phys. Rev. B **55**, R14 697 (1997); see also **57**, 11 283 (1998).
  - [5] V. Lughi, D.R. Clarke, J. Am. Ceram. Soc., to be published.
  - [6] P.W. Anderson, E.I. Blount, Phys. Rev. Lett. **14**, 217 (1965).
  - [7] J. Cai, C. Raptis, Y.S. Raptis, E. Anastassakis, Phys. Rev. B **51**, 201 (1995).

- [8] Y. Ishibashi, V. Dvorak, *J. Phys. Soc. Jpn.* **58**, 4211 (1989).
- [9] K. Negita, H. Takato, *J. Phys. Chem. Solids* **50**, 325 (1989).
- [10] A. P. Migorodsky, M. B. Smirnov, P.E. Quintard, *Phys. Rev. B* **55**, 19 (1997).
- [11] S. Fabris, A. T. Paxton, M. W. Finnis *Phys. Rev. B* **61**, 6617 (2000).
- [12] E. Anastassakis, B. Papanicolaou, I.M. Asher, *J. Phys. Chem. Sol.* **36**, 667 (1975).
- [13] P. Bouvier, H.C. Gupta, G. Lucazeau, *J. Phys. Chem. Sol.* **62**, 873 (2001).
- [14] L. A. Falkovsky, *Pis'ma v Zh. Éksp. Teor. Fiz.* **66**, 817 (1997) [*JETP Lett.* **66**, 860 (1997)].
- [15] L. A. Falkovsky, *Physics–Uspekhi* **47**, 249 (2004) [*Uspechi Fiz. Nauk* **66**, 817 (2004)].
- [16] S.-I. Tamura, *Phys. Rev. B* **30**, 849 (1984).